



GLOBAL JOURNAL OF RESEARCHES IN ENGINEERING: J
GENERAL ENGINEERING
Volume 19 Issue 5 Version 1.0 Year 2019
Type: Double Blind Peer Reviewed International Research Journal
Publisher: Global Journals
Online ISSN: 2249-4596 & Print ISSN: 0975-5861

Use of the Split Hopkinson Pressure Bar on Performance Evaluation of Polymer Composites for Ballistic Protection Purposes

By Rafael Rodrigues Dias, Iaci Miranda Pereira & Bluma Guenther Soares

Northern University Bangladesh

Abstract- This article presents a review of the split Hopkinson pressure bar uses on evaluation of polymer composites ballistic material's dynamic mechanical properties. A small introduction concerning the equipment is given, followed by a summarization of the most recent published studies relating to dynamic compressive tests used to study dynamic properties of ballistic polymeric composites such as Young's modulus, maximum stress, strain at maximum stress, tenacity and maximum strain, as well as the sensitivity of these properties to changes in the applied strain rate.

Keywords: hopkinson bar, high strain rate, ballistic composites, failure mechanisms.

GJRE-J Classification: FOR Code: 091599



USE OF THE SPLIT HOPKINSON PRESSURE BAR ON PERFORMANCE EVALUATION OF POLYMER COMPOSITES FOR BALLISTIC PROTECTION PURPOSES

Strictly as per the compliance and regulations of:



RESEARCH | DIVERSITY | ETHICS

© 2019. Rafael Rodrigues Dias, Iaci Miranda Pereira & Bluma Guenther Soares. This is a research/review paper, distributed under the terms of the Creative Commons Attribution-Noncommercial 3.0 Unported License (<http://creativecommons.org/licenses/by-nc/3.0/>), permitting all non commercial use, distribution, and reproduction in any medium, provided the original work is properly cited.

Use of the Split Hopkinson Pressure Bar on Performance Evaluation of Polymer Composites for Ballistic Protection Purposes

Rafael Rodrigues Dias ^α, Iaci Miranda Pereira ^ο & Bluma Guenther Soares ^ρ

Abstract- This article presents a review of the split Hopkinson pressure bar uses on evaluation of polymer composites ballistic material's dynamic mechanical properties. A small introduction concerning the equipment is given, followed by a summarization of the most recent published studies relating to dynamic compressive tests used to study dynamic properties of ballistic polymeric composites such as Young's modulus, maximum stress, strain at maximum stress, tenacity and maximum strain, as well as the sensitivity of these properties to changes in the applied strain rate.

Keywords: hopkinson bar, high strain rate, ballistic composites, failure mechanisms.

I. INTRODUCTION

Researches on materials applicable to individual ballistic shielding (ballistic helmet and vest), ballistic vehicles and facilities have the great challenge of increasing the resistance to impact and reducing the product weight, being, therefore, an area of great domain of the polymeric composites¹. The evaluations of the performance of these materials for ballistic armor purposes do not follow the usual standards of characterization of composites, since they are subjected to high strain rates, close to 10^4 s^{-1} , when they are hit by ammunition of small guns (revolver and pistol), as well as fragments of grenades. The drilling power of such weapons is one of the main threats to individual shielding apparatuses (ballistic helmet and vest) and vehicles⁴. Thus, the mechanical assay to be chosen in order to study the dynamic behavior of a polymeric composite for ballistic protection purposes must be capable of imposing near-to-ballistic impact deformation rates^{10, 1}.

From this perspective, the dynamic compression test in a split Hopkinson pressure bar has been considered one of the best and most indicated methods for a more detailed evaluation of the dynamic response of polymeric composites for ballistic protection, since it is robust and has a great capacity to

achieve uniaxial compression strengths in steady regime of strain rates¹¹.

The objective of the present work is to emphasize the importance of the use of the Hopkinson Bar in the evaluation of polymeric composites for ballistic applications. Initially, a brief review of the technical aspects associated with the use of the Hopkinson Bar in dynamic compression tests is presented. Subsequently, the paper presents a review of some recent scientific articles which used this equipment to study dynamic properties of ballistic polymeric composites such as Young's modulus (E), maximum stress (σ_{\max}), strain at maximum stress (ϵ_{σ}), tenacity (J) and maximum strain (ϵ_{\max}), as well as the sensitivity of these properties to changes in the applied strain rate ($\frac{d\epsilon}{dt}$).

II. SPLIT HOPKINSON PRESSURE BAR

The Split Hopkinson Pressure Bar, or simply Hopkinson Bar, is a mechanical characterization equipment used for dynamic compression tests aiming to investigate the response of a material when subjected to high strain rates ($10^2 - 10^4 \text{ s}^{-1}$)¹¹⁻¹³. The equipment was named after the work of Bertram Hopkinson in 1914, who used a cylindrical bar to experimentally estimate the pressure reached by explosive detonations and ammunition shots¹⁴. The structure currently in use, however, was conceived by Kolsky in 1949¹⁵, with some variations, mainly in the propulsion system and in the electronic signal receiving apparatus. In a broad way, it is composed of a gas chamber, an impact or, an incident bar and a transmitter bar. Figure 1 shows a schematic drawing of the equipment, with the names of its main components. In a basic description of its operation, the striker reaches the end of the incident bar driven forward by a large volume of gas suddenly released within the propulsion system.

Author α: Rafael R Dias is with Brazilian Army Technological Center. e-mail: rodrigues.dias@eb.mil.br

Author ο: Iaci Miranda Pereira is with Brazilian Army Technological Center. e-mail: iacipere@gmail.com

Author ρ: Bluma Guenther Soares is with Federal University of Rio de Janeiro. e-mail: bluma@metalmat.ufrj.br

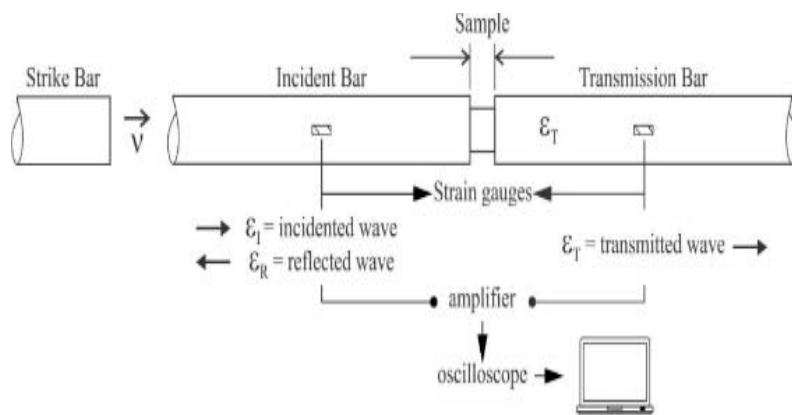


Figure 1: Isometric view of the Hopkinson Bar, with the nomenclature of the main components¹⁶.

As a consequence of the impact of the striker on the incident bar, a compressive stress wave begins its propagation. This wave, upon reaching the interface between the incident bar and the sample, has part of it reflected (voltage pulse) and the remainder is transmitted through the sample as a compression wave¹⁷. Strain-gauges are installed at half the length of each of the two bars of the equipment, capturing the vibration coming from the propagation of mechanical waves. An oscilloscope receives the signals captured, passing them on to an amplification system, which generates charts of Voltage (mV) vs. Time (ms).

incident, reflected and transmitted pulse. These values, in turn, are used in a mathematical model to calculate the tension (σ), strain (ϵ) and strain rate ($\frac{d\epsilon}{dx}$) values which act in the sample; all as a function of time.

The formulations are presented in (1) to (3):
12,13,15,18,19

$$\sigma(t) = \frac{E_b A_b}{A_a} (\epsilon_i + \epsilon_r + \epsilon_t) \quad (1)$$

$$\epsilon = \frac{-2C_b}{L_a} \int_0^t (\epsilon_i + \epsilon_r + \epsilon_t) \quad (2)$$

$$\frac{d\epsilon}{dt} = \frac{-2C_b}{L_a} (\epsilon_i + \epsilon_r + \epsilon_t) \quad (3)$$

where C_b is the speed of propagation of mechanical waves in the bar, A_b and A_a are the cross-sectional areas of the bar and sample, and E_b is the modulus of elasticity of the bar material. These equations are known as the three-wave model.

These three equations, however, were developed considering some boundary conditions which must be verified so that the values adequately represent the properties of the material. The conditions are the following^{11,13,17,20,21}:

1. The incident, transmitter and the striker bars must have the same diameter and be of the same material, being it homogeneous and isotropic. The incident and transmitter bars must have the same length. During the impacts, they must remain in the elastic regime.
2. The propagation of mechanical waves in the incident and transmitter bars is considered one-dimensional. The one-dimensional wave propagation model in bars was developed considering a semi-infinite solid medium. Since this is not in practice possible, the equipment must have sufficiently long incident and transmitter bars to ensure the predominantly one-dimensional propagation of waves. This is achieved by ensuring that the length/diameter ratio of the bars is at least equal to 20.

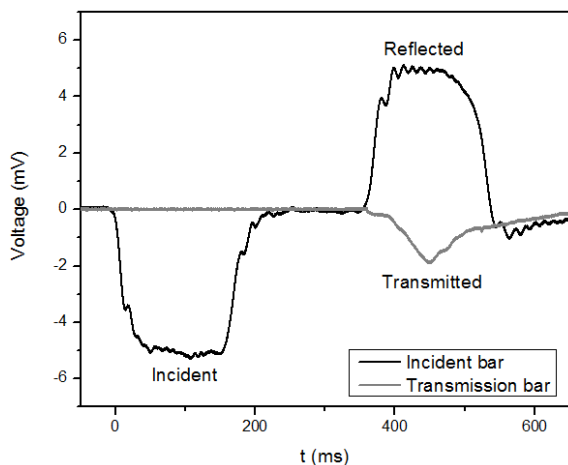


Figure 2: Typical Voltage (mV) vs. Time (ms) chart, in which the incident, reflected and transmitted pulses are identified

Figure2 shows a characteristic example of incident, reflected, and transmitted pulses. The incident and reflected pulses (in blue) are captured by the strain-gauge installed in the incident bar; while the pulse transmitted (in red) by the one installed in the transmitter bar.

The voltage values as a function of time obtained by the strain-gauges are converted into elastic strain values of the bars. We have, then, $\epsilon_i(t)$, $\epsilon_r(t)$ and $\epsilon_t(t)$ as the elastic strains generated, respectively, by the

3. The incident bar/sample and sample/transmitter bar interfaces shall be perfectly flat, with full contact between the sample and the bars.
4. The materials of the sample and bars must have close mechanical impedance. This, in turn, is the product between density and the speed of propagation of the material, (4):

$$Z = \rho C \quad (4)$$

1. The material of the sample cannot be compressible, i.e., the density of the material must not vary with the impact.
2. The test shall take place at stress equilibrium, that is, the stress applied at the incident bar/sample interface shall be convergent with the one generated at the sample/transmitter bar interface.
3. The strain rate to which each sample is subjected must be constant, that is, it cannot vary with the strain of the sample.
4. The sample must have a geometry that minimizes the interfacial friction and inertia effects, since these phenomena generate propagation of bi and/or three-dimensional waves.

Following the conditions outlined above, the mathematical model commonly used presents coherent and reliable results, but there is a natural and acceptable lag between the result obtained by pure application of the theoretical model of one-dimensional wave propagation and the practical result of a dynamic compression test. In the first case, the result would be a pulse of rectangular shape and without oscillations, while the pulse of a test has a trapezoidal profile and oscillations in its plateau (Figure 2). This is due to the propagation of mechanical waves in cylindrical bars being three-dimensional in nature, which implicates the existence of multiple wave frequencies^{19,22,23}.

III. APPLICATION OF HOPKINSON BAR AT ARMOR MATERIALS

In polymeric composites to be used in ballistic protection, the main fibers used as reinforcements are: glass, aramid and ultra-high molecular weight polyethylene (UHMWPE)^{2,3}.

Glass fibers are usually employed in structural polymer composites, whose applications in defense systems are in transportation and constructions susceptible to ballistic impacts and/or wave propagations from explosions, such as bunkers, aircrafts and military vehicles^{1,4,5}. Aramid fibers were developed in 1965 and are routinely used in individual ballistic shielding apparatuses (helmets and ballistic vests), and can also be used in collective shielding apparatuses (military vehicles, utilitarian vehicles and facilities), with DuPont (Kevlar[®]) and Teijin (Twaron[®]) as

its main producers⁶⁻⁸. Ultra high molecular weight polyethylene (UHMWPE) fibers, in turn, were developed in the late 1980s and began to excel in the area of individual ballistic vests during the 1990s⁹. Currently, the prepregs of UHMWPE fibers already dominate individual shielding markets that once were dominated by the aramid fibers, given that they also have high modulus of elasticity and tenacity, but a considerably lower density^{3,5}. Its most known producers are DSM (Dyneema[®]) and Honeywell (SpectraShield[®]).

Table 1 compiles the articles addressed in this work, listing the authors of the articles, the composites studied, the processing used and the strain rates imposed to the material.

Govender et al.³⁷ tested, in a Hopkinson Bar, glass fiber/vinyl ester resin composites, comparing the results of σ_{max} with those of the quasi-static compression test, identifying an increase of 10%. Failure analysis of the samples under optical microscopy indicated delamination, fracture of fibers and fracture plane at 45° in relation to the longitudinal axis.

Tasdemirci et al.³⁸ impacted samples of glass fiber/PS composites, evaluating E and σ_{max} to compare the dynamic and quasi-static behaviors, in longitudinal, transverse and across thickness directions. In all of these, the properties cited increased significantly under dynamic assay.

Zainnudin et al.³⁹ exposed glass fiber/epoxy (pure and nanostructured) composites to interspersed UV radiation/condensation treatments with different durations. The dynamic properties, E and σ_{max} , decreased as the UV/condensation treatment time increased. Compared with equivalent treatment conditions, the nanostructured matrix samples had superior properties than pure matrix composites, under all conditions, which was attributed to better interfacial adhesion, and therefore less delamination in comparison with the other compositions.

Kim et al.⁴⁰ produced glass fiber/polyester (pure and CNT) and glass fiber/polyurethane (pure and CNT) composites. Dynamic compression tests were used to compare the impact absorption capacity of each composite, with and without the treated fiber layers, and found that the greatest ϵ_{max} and J were obtained by the glass fiber/polyurethane/CNT composite.

Arbaoui et al.⁴¹ studied the compressive properties in the plane (fiber-weft direction), E, σ_{max} and ϵ_{σ} , of glass fiber woven fabric/vinyl ester resin composites, of bi- or three- dimensional woven fabrics. The 3D woven fabric composites showed superior properties at all rates employed, especially for σ_{max} , in which the 2D woven fabric showed a decline in the highest rates employed.

Tarfaoui et al.⁴² processed glass fiber/epoxy composites, presenting in a dynamic test a reasonable

sensitivity to the increase of $\frac{d\varepsilon}{dt}$, when displaying greater ε_{\max} and J whilst receiving greater impact pressures. Using high-speed infrared camera, the authors verified that the impact energy was dissipated through matrix rupture, delamination and fiber breakage; mechanisms which became more present as $\frac{d\varepsilon}{dt}$ increased.

Researchers Woo and Kim⁴³ processed aramid/phenolic resin prepregs, which presented, in tests of dynamic compression, sensitivity to small variations of $\frac{d\varepsilon}{dt}$, with linear growth of σ_{\max} (233%) and J (211%). The variable ε_{σ} of the composite, on the other hand, presented a slight reduction (16%) with the increase of $\frac{d\varepsilon}{dt}$. SEM images and acoustic emission signals indicated matrix rupture, delamination, fiber tearing and rupture as the main failure mechanisms. The researchers concluded that with the increase of the impact energy, the samples presented fragile fractures in greater volume and faster, reducing its strain capacity, justifying the reduction of ε_{σ} . In the subsequent work by the same authors⁴⁴, a hybrid woven fabric composed of carbon fibers (weft) and para-aramid (warp) was used, with the same resin and same fiber/matrix ratio as Woo and Kim⁴³. The properties showed sensitivity to variations of $\frac{d\varepsilon}{dt}$, but more discreet.

The σ_{\max} , however, were 1.6x higher than those obtained in the previous study⁴³. In addition to all failure mechanisms present in the aramid fiber composite, there was a fragile fracture of the carbon fibers, which contributed to increase the impact resistance of the material, expressed in the increase of σ_{\max} .

Chouhan et al.⁴⁶ worked with aramid/PP-co-AM (10%) composites, testing samples with different amounts of fabric layers (16, 24 and 30) and therefore different e/d ratios, in order to study the quality of the results obtained in each geometry, observing the best dynamic properties in the 24-layer composite. Kapoor et al.⁴⁵, in turn, tested, at 6 different strain rates, the composite that presented the best conditions in Chouhan et al.⁴⁶, developed equations for the dynamic properties as a function of $\frac{d\varepsilon}{dt}$ and compared the results with those of Woo and Kim⁴³. The composite presented second-order growth of J and linear growth of ε_{σ} , therefore greater than the aramid/phenolic resin tested in⁴³. The higher impact absorption capacity of the material was associated with the ductility of the thermoplastic matrix and the higher fiber/matrix adhesion ensured by the presence of maleic anhydride.

Bandaru et al.⁴⁷ manufactured aramid/PP and aramid/basalt/PP composites, testing all of them on a Hopkinson Bar. The composite of hybrid woven fabric obtained superior results of E and σ_{\max} due to higher fiber/matrix adhesion of the basalt/PP composite. The fragility of the basalt, however, made the hybrid

composites present a decrease in ε_{σ} with the increase of $\frac{d\varepsilon}{dt}$, whereas the homogeneous aramid/PP composite showed growth in this value in the same situation, corroborating the results obtained with two-dimensional fabrics^{45,46}.

Qian et al.⁴⁸ tested samples of aramid/PA₆ composite plates, with different fiber/matrix ratios, analyzing the response of each material to the increase in the impact energy, as well as the influence of the variation in the thickness/diameter ratio on the dynamic properties of the material. They concluded that, regardless of the composition, all of them presented sensitivity to $\frac{d\varepsilon}{dt}$ and compositions with higher fiber volume presented higher E and σ_{\max} ; and smaller ε_{\max} .

Table 1: Compilation of the studied authors, their materials, processes employed and observations on the tests

References	Composites studied	Processing	Strain Rates (s ⁻¹)	Observations
Govender et al. ³⁷	Plain glass fiber fabric E/vinyl ester (Derakane® 8084)	RTM	~ 520	Use of a conical striker to reduce the variation of the strain rate between tests.
Tasdemirciet al. ³⁸	Quadri-axial glass fiber Fabric E [0/45/90/-45]/polyester (Crystic® 702PAX)	VARTM	~ 900	The tests were recorded by a high-speed camera in order to study the strain mechanisms and to compare them with those presented in the finite element program developed by the authors.
Zainuddin et al. ³⁹	Unidirectional non-woven glass fiber E (FiberGlast) / epoxy (S-15®) / montmorillonite nanofiller (Nanomer® I. 28E)	RTM	382 440 510	The composites were submitted to treatments that interspersed 4h of UV radiation and 4h of condensation, with different durations (5, 10 and 15 days).
Kim et al. ⁴⁰	Plain glass fiber fabric / PS / CNT Plain Fiberglass Fabric / PU / CNT	Autoclaving	700	Composites with 13 layers of pure glass fiber fabric and composites with 3 of the 13 layers of fabrics reinforced by vertically aligned carbon nanotubes (VACNT) were processed.
Arbaoui et al. ⁴¹	Bi-dimensional and three-dimensional glass fiber fabrics E (EADS composites) / vinyl ester (DION® 9102)	Vacuum resin infusion	224-882	The three-dimensional composites employed are composed of 6% in volumes of polystyrene fibers oriented in the Z direction.
Tarfaii et al. ⁴²	Unidirectional non-woven glass fiber E/Epoxy (EPOLAM®)	Vacuum resin infusion	285 - 1430	Use of thermocouples and high-speed infrared cameras to monitor the temperature change of the samples during the test.
Woo and Kim ⁴³	758 HPP® (acronym of Helmet Phenolic Prepreg, from DuPont)	Hot Compression	1182 1322 1460	Use of the acoustic emission technique to evaluate the failure mechanisms of the composite during the dynamic compression test.
Woo and Kim ⁴⁴	Twill carbon fibers woven T-300® and aramid K49® (DuPont) / phenol-formaldehyde	Hot Compression	1007 1485 1927	Tests on the Hopkinson Bar were used to determine the best thickness/diameter ratio for the composite tested.
Kapoor et al. ⁴⁵	Plain aramid fiber fabric K29® (Dupont) / polypropylene-maleic co-anhydride (PP-co-AM)	Vacuum-assisted hot compression	2101 - 9965	Maleic anhydride was used as a compatibilizer in the polypropylene matrix to increase the fiber/matrix adhesion.
Chouhan et al. ⁴⁶	Kevlar® plain aramid fiber fabric/ Basalt fiber/ Polypropylene	Vacuum-assisted hot compression	1370-4264	Use of three-dimensional hybrid fabrics of para-aramid/basalt in the ballistic plate processing.
Qian et al. ⁴⁸	Plain aramid fiber fabric	Hot	456	Processing of composites with different

	K29®/polyamide (PA ₆)	Compression	782 1153	fiber/matrix ratios, investigating the influence of this parameter on the dynamic results.
Cao et al. ⁴⁹	Kevlar plain aramid fiber woven® / Non-Newtonian Fluid	Hand Layup	4318 6438 8702	The feasibility of a non-Newtonian fluid as a composite matrix to be subject to high strain rates was verified.
He et al. ⁵⁰	Plain aramid fabric K129®/Non-Newtonian Fluid/Stiffening Gel	Hand Layup	4318	Use of a stiffening gel to accommodate the non-Newtonian fluid, as a way of better distributing it through the fibers.
Pagnocelli et al. ¹⁶	Plain aramid fiber fabric K29® / Vinyl ester (Derakane® 411-350)	MTR	2000	Samples were drawn from five different areas of 300 mm x 300 mm ballistic plates using the dynamic assay to verify the homogeneity of plate impact response.
Rabbi et al. ⁵¹	Kevlar® plain aramid fiber fabric/epoxy Kevlar® auxetic woven/epoxy	Vacuum infusion	1200-3300	Processing of composites with auxetic aramid woven and nanocomposite epoxy resin / Nylon short fibers.
Shaker et al. ⁵²	Dyneema H62® / LDPE Dyneema H5T® / LDPE Twaron CT 736® (Teijin)/LDPE ArtecRussian® /LDPE K49®/LDPE	Autoclaving	1000-8000	Woven and non-woven aramid and/or UHMWPE were used in the composites co-processing.
Shi et al. ⁵³	UD75® prepreg (ZhongtaiInc)	Hot Compression	430 840 1200	Processing of the composites by turning the adjacent blades at specific angles, in order to obtain different directions of fibers.
Parker and Ramesh ⁵⁴	Dyneema HB80® prepreg (DSM)	Hot Compression	3500	Study of different processing pressures and their effect on the dynamic response of the material.
Zhu et al. ⁵⁵	UHMWPE/Polyurethane	Hot Compression	1000-3000	Hygrothermal treatment performance, at different execution times, and comparison with the resistance to impact of the untreated composite.
Asija et al. ⁵⁶	GoldShield® (Honeywell) treated in non-Newtonian fluid	Hot Compression	3000-10000	Prepregs were subjected to treatment in non-Newtonian fluid prior to processing.
Asija et al. ⁵⁷	GoldShield® (Honeywell)/polymer foam film soaked with non-Newtonian fluid	Hot Compression	3000-10000	Use of a foam film soaked with a non-Newtonian fluid, arranged between the prepregs to disperse the liquid through the composite.
Fin et al.	Tensylon® (DuPont) Plain aramid fiber woven K29®/Ethylene Vinyl Acetate (EVA)	Autoclaving	~2050	UHMWPE non-woven co-processing and para-aramid/EVA woven in three different ratios (25/75, 50/50 and 75/25, respectively), comparing the results of dynamic impacts with the respective homogeneous composites.

Cao et al.⁴⁹ studied mechanical and energy absorption properties of aramid/non-Newtonian fluid by subjecting composites of different fiber/matrix ratios to the same impact energy. Higher percentages of non-Newtonian fluid ensured an increase of E and J, which was attributed to the ability of the matrix to, once it adhered to the fibers, hinder the interlaminar shear and delamination of the composite. Noting this result, He et al.⁵⁰ modified the research material using as a matrix a stiffening gel soaked with a non-Newtonian fluid. In comparison to ⁴⁹, the values of E did not present significant variations and there was a 10% decrease in J.

Pagnocelli et al.¹⁶ used the dynamic compression test on samples taken from 5 different regions of aramid/vynil-ester ballistic plates in order to verify if the distribution of the matrix through the fabrics occurred homogeneously during processing. The authors used σ_{\max} and J in this comparison, verifying that the peripheral regions obtained statistically equal properties, while the central region obtained mechanical property values 20% lower, an event associated to the fact that this region accumulated a larger volume of resin, making it fragile.

Rabbi et al.⁵¹ used the tests in a Hopkinson Bar to compare two aramid/epoxy composites: one flat and one auxetic woven fabric. In both cases, the epoxy resin was impregnated with short Nylon fibers®, to study the dynamic responses of composites with or without short fibers in the matrix. The authors observed that all composites showed an increase in the values of ϵ_{\max} and σ_{\max} as a function of $\frac{d\epsilon}{dt}$, and this sensitivity was higher for plane aramid/pure epoxy resin fabric composites. For the composite of auxetic fabric, however, the nanostructured resin was more efficient than the pure one. This was due to the greater spacing in the auxetic fabric, with the short fibers being able to penetrate through the fabric and remain oriented along the direction of impact, increasing the strength of the composite.

Shaker et al.⁵² tested homogeneous and hybrid composites of several aramid and UHMWPE fibers, all processed with LDPE matrix. The stress-strain and J behaviors were studied by the researchers, who verified that, in all $\frac{d\epsilon}{dt}$, the unidirectional/LDPE homogeneous composite CT736® showed the highest σ_{\max} values, while the hybrid composite CT736® fabric + Artec® fabric/LDPE presented the best results of J.

Shi et al.⁵³ investigated the energy absorption variation of UHMWPE/LDPE composites by modifying the fiber angulation by rotating the prepreg lamina in relation to the adjacent one. The researchers observed a significant increase in J in multi-oriented fiber composites.

Parker and Ramesh⁵⁴ used the Hopkinson Bar in UHMWPE/polyurethane composites, Dyneema HB80®, processed via compression at different pressures, 1 ksi and 5 ksi. The composite submitted to processing at higher pressure presented higher stiffness, E, and also larger J.

Zhu et al.⁵⁵ subjected to dynamic compression tests samples of UHMWPE/polyurethane which underwent hydrothermal treatment. The σ_{\max} of samples treated for 12 days increased with $\frac{d\epsilon}{dt}$; the opposite occurred with samples that underwent 24 days of treatment. Effects of matrix plastifying dominated the dynamic compression properties for the first 12 days, while the degradation of the fiber/matrix interface and the expansion of the internal gaps played more important roles in samples that underwent 24-hour treatment.

Asija et al.⁵⁶ tested ballistic prepreg Golden Shield® composites, treated for 4 hours in non-Newtonian fluid, comparing it with the untreated composite. Both had sensitivity to $\frac{d\epsilon}{dt}$; and the treated composite presented steep growth of σ_{\max} and J, while the pure composite presented softer growths. The silica nanoparticles present in the fluid, when lodging between the fibers require greater efforts for the occurrence of failure mechanisms such as interlaminar and interfiber shear. The same group⁵⁷, in a subsequent work, used a PP-co-AM polymeric foam film to absorb the non-Newtonian fluid, with further co-processing with GoldShield® ballistic prepreps. The results in the dynamic compression test of these composites were much lower than in the previous work, since there was no efficient interaction of the non-Newtonian fluid with the UHMWPE fibers, only with the PP-co-AM foam film.

Fin et al. co-processed Tensylon® and aramid/EVA prepreps in 3 different compositions, in addition to their respective homogeneous composites. Subject to dynamic compression tests, all at the same rate, the composites showed linear growth of σ_{\max} and J as a function of the increase of the percentage of Tensylon® layers; and the homogeneous composite of this material presented, therefore, the most expressive results.

IV. CONCLUSION

It can be understood from this review that the dynamic compression test in split Hopkinson pressure bar is an efficient method for evaluating the efficiency of ballistic polymeric composites, although there is still limited literature on the subject. Whether comparing it to the quasi-static regime or using several dynamic tests, the authors investigated the effect of an increase in the strain rate ($\frac{d\epsilon}{dt}$) in compression properties. The ballistic composites are sensitive to this parameter, presenting

an increase in Maximum Stress (σ_{max}) and Tenacity (J). The comparison between articles indicates that composites with thermoplastic matrices tend to have growing properties related to strain (ϵ_{σ} and ϵ_{max}), while the thermo rigid composites have decreasing properties as higher rates are applied. The authors also sought to observe and understand the several failure mechanisms during impact, and matrix rupture, delamination and fiber rupture were highlighted.

REFERENCES RÉFÉRENCES REFERENCIAS

- Bhatnagar, A. *Lightweight ballistic composites*. (CRC, 2006).
- Chawla, K. K. *Composite Materials: Science and Engineering*. (Springer, 2012).
- Pegoretti, A., Traina, M. & Vlasblom, M. in *Handbook of Properties of Textiles and Technical Fibres* (ed. Bunsell, A. R.) 638–991 (The Textile Institute Book Series., 2018).
- Crouch, I. in *The Science of Armour Materials*. (ed. Crouch, I.) 1–54 (Elsevier Ltd., 2017).
- Hazell, P. J. *Armour: Materials, Theory and Design*. (CRC Press., 2016).
- Hamouda, A. M. S., Sohaimi, R. M., Zaidi, A. M. A. & Abdullah, S. in *Advance in military textiles and personnel equipments*. (ed. Sparks, E.) 103–138 (Woodhead Publishing, 2012).
- Rebouillat, S. in *Advanced Fibrous Composite Materials for Ballistic Protection*. (ed. Chen, X.) (Woodhead Publishing., 2016).
- Jackson, T. & Samanta, S. Characterization of Kevlar Fiber and Its Composites : A Review. *Mater. Today Proc.* 2, 1381–1387 (2015).
- Crouch, I. G., Sandlin, J. & Thomas, S. in *The Science of Armour Materials*. (ed. Crouch, I.) 203–268 (Elsevier Ltd., 2017). doi:10.1016/B978-0-08-100704-4.00005-0
- Vaidya, U. K. in *Impact Engineering of Composite Structures*. (ed. Abrate, S.) 97–192 (Springer Wien., 2011).
- Gray III, G. T. (Rusty). in *ASM Handbook Vol. 8 - Mechanical Testing and Evaluation*. (eds. Kuhn, H. & Medlin, D.) 1027–1046 (ASTM International., 2000).
- Meyers, M. *Dynamic Behavior of Material*. (John Wiley and Sons, Inc., 1994).
- Chen, W. W. & Song, B. *Split Hopkinson (Kolsky) Bar: Design, Testing and Applications*. (Springer, 2011).
- Hopkinson, B. A Method of Measuring the Pressure Produced the Detonation Explosives or by the Impact of Bullets. *Philos. Trans. R. Soc. AA* 213, 437–456 (1914).
- Kolsky, H. An investigation of the mechanical properties of materials at very high rates of loading. *Proc. Phys. Soc. London, Sect. B62*, 676–700 (1949).
- Pagnoncelli, M. *et al.* Mechanical and ballistic analysis of aramid/vinyl ester composites. *J. Compos. Mater.* 0, 1–11 (2017).
- Field, J. E., Walley, S. M., Proud, W. G., Goldrein, H. T. & Siviour, C. R. Review of experimental techniques for high rate strain and shock studies. *Int. J. Impact Eng.* 30, 725–775 (2004).
- Davies, E. D. H. & Huntet, S. C. The dynamic compression testing of solids by the method of the split Hopkinson pressure bar. *J. Mech. Phys. Solids* 11, 155–179 (1963).
- Follansbee, P. S. & Frantz, C. Wave Propagation in the Split Hopkinson Pressure Bar. *J. Eng. Mater. Technol.* 105, 61–66 (1983).
- Gama, B. A., Lopatnikov, S. L. & Gillespie Jr., J. W. Hopkinson Bar Experimental Technique : A Critical Review. *Appl. Mech. Rev.* 57, 223–250 (2004).
- Wu, X. & Gorham, D. Stress Equilibrium in the Split Hopkinson Pressure Bar Test. *J. Phys.* IV, C3-91-C3-96 (1997).
- Gorham, D. A. A numerical method for the correction of dispersion in pressure bar signals. *J. Phys.* IV. 477–479 (1983).
- Ren, L., Larson, M., Gama, B. A. & Gillespie, J. W. *Wave Dispersion in Cylindrical Tubes : Applications to Hopkinson Pressure Bar Experimental Techniques*. (2004).
- Hosur, M. V, Alexander, J., Vaidya, U. K. & Jeelani, S. High strain rate compression response of carbon / epoxy laminate composites. *Compos. Struct.* 52, 405–417 (2001).
- Naik, N. K. & Kavala, V. R. High strain rate behavior of woven fabric composites under compressive loading. *Mater. Sci. Eng.* 474, 301–311 (2009).
- Dias, R. R., Sousa, S. D., Patrício, P. S. O. & Pereira, I. M. Influence of thickness/diameter ratio on strain hardening behavior of high molecular weight polyethylene after dynamical compressive tests using Hopkinson pressure bar. in *30th International Symposium on Ballistics*. 2629–2640 (Destech Publication., 2017). doi:10.12783/ballistics2017/17047
- Brown, E. N. *et al.* Influence of Molecular Conformation on the Constitutive Response of Polyethylene : A Comparison of HDPE, UHMWPE and PEX. *Exp. Mech.* 47, 381–393 (2007).
- Naik, N. K., Pandya, K. S., Ponthnis, J. R. & Gelu, T. A. Revisiting Kolsky bar data evaluation method. *Compos. Struct.* 111, 446–452 (2014).
- Pan, Y., Chen, W. & Song, B. Upper Limit of Constant Strain Rates in a Split Hopkinson Pressure Bar Experiment with Elastic Specimens. *Exp. Mech.* 34, 440–446 (2005).
- Naik, N. K., Ch, V. & Kavala, V. R. Hybrid composites under high strain rate compressive loading. *Mater. Sci. Eng.* 47, 87–99 (2009).

31. Gorham, D. AN EFFECT OF SPECIMEN SIZE IN THE HIGH STRAIN RATE COMPRESSION TEST. *J. Phys. IV*, C3-411-C3-418 (1991).
32. Zhong, W. Z. *et al.* Influence of interfacial friction and specimen configuration in Split Hopkinson Pressure Bar system. *Tribol. Int.* 90, 1–14 (2015).
33. Iwamoto, T. & Yokoyama, T. Effects of radial inertia and end friction in specimen geometry in split Hopkinson pressure bar tests: A computational study. *Mech. Mater.* 51, 97–109 (2012).
34. Arjun, S. & Sen, O. Effect of Specimen Size in the Kolsky Bar. *Procedia Eng.* 10, 2663–2671 (2011).
35. Lindholm, U. S. Some experiments with the split Hopkinson pressure bar. *J. Mech. Phys. Solids* 12, 317–335 (1964).
36. Samanta, S. K. DYNAMIC strain OF ALUMINIUM AND COPPER AT ELEVATED TEMPERATURES. *J. Mech. Phys. Solids* 19, 117–135 (1971).
37. Govender, R. A., Louca, L. A., Pullen, A., Fallah, A. S. & Nurick, G. N. Determining the through-thickness properties of thick glass fiber reinforced polymers at high strain rates. *J. Compos. Mater.* 46, 1219–1228 (2012).
38. Tasdemirci, A. *et al.* Experimental and Numerical Investigation of High Strain Rate Glass/Polyester Composite. *Procedia Eng.* 10, 3068–3073 (2011).
39. Zainuddin, S., Hosur, M. V., Barua, R. & Kumar, A. Effects of ultraviolet radiation and condensation on static and dynamic compression behavior of neat and nanoclay infused epoxy/glass composites. *J. Compos. Mater.* 45, 1901–1918 (2011).
40. Kim, K. *et al.* Dynamic Mechanical Analysis and High Strain-Rate Energy Absorption Characteristics of Vertically Aligned Carbon Nanotube Reinforced Woven Fiber-Glass Composites. *J. Nanomater.* 7 pages (2015). doi:10.1155/2015/480549
41. Arbaoui, J., Tarfaoui, M., Bouery, C., El, A. & Alaoui, M. Comparative study of mechanical properties and damage kinetics of two- and three-dimensional woven composites under high-strain rate dynamic compressive loading. *Int. J. Damage Mech.* 25, 878–899 (2016).
42. Tarfaoui, M., Moumen, A. El & Yahia, H. Ben. Damage detection versus heat dissipation in E-glass / Epoxy laminated composites under dynamic compression at high strain rate. *Compos. Struct.* 186, 50–61 (2018).
43. Woo, S. & Kim, T. High-strain-rate impact in Kevlar-woven composites and fracture analysis using acoustic emission. *Compos. Part B* 60, 125–136 (2014).
44. Woo, S. & Kim, T. High strain-rate failure in carbon/Kevlar hybrid woven composites via a novel SHPB-AE coupled test. *Compos. Part B* 97, 317–328 (2016).
45. Kapoor, R., Pangenji, L., Kumar, A. & Ahmad, S. High strain rate compression response of woven Kevlar reinforced polypropylene composites. *Compos. Part B* 89, 374–382 (2016).
46. Chouhan, H., Asija, N., Amare, S. & Bhatnagar, N. Effect of Specimen Thickness on High Strain Rate Properties of Kevlar/Polypropylene Composite. *Procedia Eng.* 173, 694–701 (2017).
47. Bandaru, A. *et al.* Characterization of 3D angle-interlock thermoplastic composites under high strain rate compression loadings. *Polym. Test.* 62, 355–365 (2017).
48. Qian, X., Wang, H., Zhang, D. & Wen, G. High strain rate out-of-plane compression properties of aramid fabric reinforced polyamide composite. *Polym. Test.* 53, 314–322 (2016).
49. Cao, S. *et al.* High strain-rate dynamic mechanical properties of Kevlar fabrics impregnated with shear thickening fluid. *Compos. Part A* 100, 161–169 (2017).
50. He, Q. *et al.* Impact resistance of shear thickening fluid/Kevlar composite treated with shear-stiffening gel. *Compos. Part A* 106, 82–90 (2017).
51. Rabbi, F., Chalivendra, V. & Kim, Y. Dynamic constitutive response of novel auxetic Kevlar/epoxy composites. *Compos. Struct.* 195, 1–13 (2018).
52. Shaker, K., Jabbar, A., Karahan, M., Karahan, N. & Nawab, Y. Study of dynamic compressive behaviour of aramid and ultrahigh molecular weight polyethylene composites using Split Hopkinson Pressure Bar. *J. Compos. Mater.* 51, 81–94 (2017).
53. Shi, B., Sun, Y., Chen, L. & Li, J. Energy Absorption of Ultra-High Molecular Weight Polyethylene Fiber-reinforced Laminates at High Strain Rates. *Appl. Mech. Mater.* 35, 1532–1535 (2010).
54. Parker, J. & Ramesh, K. T. Effect of Microstructure on the Transverse Compressive Strength of UHMWPE Composites at High Strain-rates. 1 (2016).
55. Zhu, L., Li, Y., Zhu, X. & Zhu, Z. Compressive mechanics and failure mechanism for UHMWPE fiber reinforced composite laminated under hygrothermal environment. in *International Conference of Composite Materials.* 20–25 (2017).
56. Asija, N., Chouhan, H., Gebremeskel, S. A., Singh, R. K. & Bhatnagar, N. High strain rate behavior of STF-treated UHMWPE composites. *Int. J. Impact Eng.* 110, 359–364 (2017).
57. Asija, N., Chouhan, H., Gebremeskel, S. A. & Bhatnagar, N. Impact response of Shear Thickening Fluid (STF) treated ultra high molecular weight poly ethylene composites – study of the effect of STF treatment method. *Thin Walled Struct.* 126, 16–25 (2018).